5/9-89

N94- 35561

TDA Progress Report 42-117

May 15, 1994

A New Presentation of Complex Voltage Data for Goldstone Radar Astronomy

S. D. Howard
Communications Systems Research Section

A presentation method similar to a vector field display or a data-based grid has been used to visualize complex voltage test data taken over multiple subchannels. Unlike simple plots of all data points on the complex plane, the position of the data in the time series is part of the presentation, providing additional information to aid in fault isolation during readiness testing. The "phase–magnitude" presentation, as it has come to be called, was designed for the demands of real-time data acquisition and processing with remote monitoring over low bandwidth communication links.

I. Introduction

A new real-time presentation of complex voltage data taken over multiple subchannels has been added as a display option to the Goldstone Solar System Radar ranging system. The new voltage data presentation was adapted from a design devised for complex interferometry data [1], referred to as a "phase–magnitude" presentation. It is similar in appearance to a vector field display or a data-based grid [2]. The voltage phase–magnitude presentation was intended to improve the effectiveness of readiness testing by enabling engineers to discover and correct defects before the data from an observation could be degraded or lost during acquisition due to component failures in the special-purpose signal processing hardware.

The ranging data-acquisition system was initially developed as a rapid prototype. Over the past 5 years, the software has undergone several significant upgrades to enhance reliability, add functionality, improve performance, and correct defects. An early example of one of these reengineering episodes is described in [3]. The most recent upgrade, a replacement of the software that manages the real-time data display, made complex voltage data available to the display and provided an extensible software architecture for experimenting with new methods of visualizing radar data. With the exception of the earliest version of the ranging system (1985) where power profiles were summed from complex voltage data and displayed, prior to the upgrade conjectures about the state of the system during readiness testing were made from integrated power spectra shown in the delay–Doppler display.

Readiness testing in the radar data-acquisition system typically takes the form of local loop-back testing. During a loop-back test, a point-source test signal is injected into the data-acquisition system before the analog-to-digital converters. Incoming test data are then digitized, autocorrelated, coherently summed, transformed to the frequency domain, detected by taking the magnitude squared, incoherently summed, and displayed in real time. The frequency and time delay of the test signal can be set by the operator. Engineers examine the real-time display as

Appendix

Interferometry Data Type Description

Let $(t_1, \ldots, t_n)_{r,c}$ represent a vector of complex voltage samples, t_i taken on a channel $c, c = 0, \ldots, C-1$, where C is the number of complex channels for range gate $r; r = 0, \ldots, R-1$, where R is the number of range gates. The variable n is a power of 2, limited by implementation to be between 64 and 2048.

The expression $(f_1, \ldots, f_n)_{r,c}$ represents the result of applying a discrete Fourier transform to $(t_1, \ldots, t_n)_{r,c}$.

The complex spectra from selected channels l and m are combined by applying a complex conjugate multiply to corresponding elements from both spectra:

$$X_{r,l \times m} = ({f^*}_{1,r,m} f_{1,r,l}, \ldots, {f^*}_{n,r,m} f_{n,r,l})$$

Crosspower spectra for channels l and m are then computed for all range gates r in the given configuration to form the interferometry data structure.

a succession of data records is received, usually at about 30-sec intervals, for evidence of continuous or intermittent defects.

The interpretation of integrated power spectra of test data had two difficulties. First, in the hardware that digitizes, correlates, and sums data, failures occurred in the time domain. Interpretation of the data in the frequency domain was removed from the direct connection to the problem. Second, although integration reduced system noise and data rates during data acquisition, it could also reduce the visibility of intermittent defects during testing. The new presentation addressed these difficulties by presenting a user-selectable subset of time series data on multiple subchannels at selected intervals; integration was optional.

Experimentation with new data visualization methods had been a design goal of the ranging system display upgrade, so the incorporation of this presentation method into the ranging system was also another demonstration of the feasibility of an extensible research and development (R&D) software architecture.

II. Design

The radar test data shown in the phase–magnitude presentation in Fig. 1 are a series of complex voltage samples. As in the case of the interferometry presentation, each phasor represents one complex data point. Square areas representing the complex plane for each data point are nonoverlapping to avoid the visual confusion that might be caused by intersecting phasors. The in-phase and quadrature components correspond to the horizontal and vertical dimensions, respectively. Both phasor components are scaled to the maximum displayed in-phase or quadrature component. The rows in the phasor grid carry samples for a given subchannel or range gate. Columns are time samples taken within each subchannel; time increases from left to right. Only a region of the data is shown at any given time; however, the operator may change the region in the display at any time during the test.

To illustrate the effect of various frequencies on the appearance of the test signal in this kind of presentation, a series of local loop-back tests taken with the ranging system in a typical Mercury configuration (oversampled with a 4.0-μsec range resolution) is shown in Fig. 2. Because the configuration is oversampled, the test signal can be seen in range gates adjacent to range gate 11. As time increases from left to right, the phasor angle advances or retards, depending on the frequency of the test signal. The length of the phasor should be constant. In practice, since a small positive frequency is usually used to offset the point-source test signal from dc, a display similar to the 5-Hz case in Fig. 2(d) has become a familiar signature of good test data when viewed with the phase–magnitude presentation.

System noise is shown in Fig. 3. Gaussian noise looks random in the display. One of the early concerns about using a data-based grid in the design of the data graphic was that the viewer might be induced to perceive a pattern in the graphic when no such relationship actually existed in the data. Experience with the display has greatly reduced that concern, although assertions about subjective experience are difficult to quantify. In practice, engineers have been able to recognize and challenge subtle differences between pure system noise and noise that accidentally included other artifacts.

Expert test engineers rely on their ability to recognize patterns and subtle mismatches in patterns through visual, auditory, and sometimes tactile modes when they evaluate the behavior of complex systems. One of the goals of the phase–magnitude design was to provide not only readily interpretable signs about the basic state of the system but additional visual support for complex information gathering and decision making as well. A test engineer, experienced with the system and the presentation, should be able to glance at the display and immediately identify the appearance and source of familiar problems. In addition, if the problem did not match some previous experience, the display ought to provide a good representation of the available information to assist the troubleshooting process.

A common method of presenting sets of complex data samples graphically is to simply plot them all on a single complex plane. The advantage of this approach is that many data points can be included; this is useful for indicating whether or not a failure or anomaly has occurred. The disadvantage is that the association between each data point and its position in the time series is not defined by the graphic. The presence of a number of subchannels in the ranging system data further complicates the use of this kind of approach. The design of the new data graphic, by contrast, accepted the reduction in the number of data points plotted, in favor of retaining information about the position of data points in the time series. Since rapid fault isolation is the goal, the time dimension in the phase–magnitude presentation can show when the anomaly is occurring, giving additional information about the origin of the problem.

III. Experience

The first diagnostic use of the new method showed a defect that was later traced to a memory chip failure in a correlator–accumulator module. A printout of a typical display is shown in Fig. 4. Instead of the expected Gaussian noise display, similar to Fig. 3, a few large negative in-phase values in range gates 173, 185, and 187 dominated. The large negative values did not usually persist in fixed time-sample locations from data record to data record, as Fig. 4 might suggest, but occurred in various time-sample locations throughout the range gate, indicating that the defect was probably occurring after sampling. A display like Fig. 4 now suggests that this kind of failure needs to be investigated; memory chip failures are among the more frequently encountered failures in the radar modules.

The second experience, illustrated by the printout of the display in Fig. 5, alerted sustaining engineering to an unsuspected problem. Since the system is set for oversampling in this configuration, the test signal is expected to spread over three range gates. However, the test signal also apparently drifts forward in range from gates 10, 11, and 12 to gates 8, 9, and 10 in the first 12 time samples. After a timing adjustment of the baud-integrating analog-to-digital converters that supply data to digital channel 1, the test results showed a normal signal in range gates 10, 11, and 12, similar to that in Fig. 1.

IV. Conclusions

The key elements of the design were probably the retention of the time dimension in the data graphic and the acceptability of being able to view only selected regions of the data record at any given time. However, performance and aesthetics were also factors in the decision to incorporate this display method into the standard set. Because this design is an adaptation of the interferometry design, it places a low processing burden on the real-time system and retains the acceptable performance characteristics that allow remote monitoring over 9600-bps communication links. The display of a typical loop-back test with a small frequency offset exhibits a varying but symmetrical and aesthetically pleasing pattern. This was a fortuitous result. Unsatisfactory outcomes either in performance or in overall graphic design would have argued against pursuing this method as an operational tool.

Several measurements of how well the presentation conveys information might be of interest if the opportunity for more quantitatively based testing arises. First, some measurement might be made of the ability of users to identify a printout as being either of Gaussian system noise or noise combined with dc. There is probably a threshold below which users cannot distinguish the presence of dc. That threshold may vary among users and with experience. Second, it should also be possible to test the ability of users to identify printouts as being either from normal loop-back tests or from tests showing captured or induced system defects. If printouts are identified as being of system defects, then the user might be asked to identify a prioritized list of candidate problem sources. Again, some variation in ability among users is expected.

The initial informal evaluation of the voltage phase-magnitude presentation contributed to the preparation for the successful observations of asteroid 4179 Toutatis and of Mars in December 1992. Additional informal assessments of the power of this representation of complex voltage data to carry relevant information to users will continue as new situations arise in testing.

Acknowledgments

The author thanks Carl Franck and Ray Jurgens for assistance in setting up calibrated loop-back tests at DSS 14. Ron Winkler, Carl Elston, Larry Snedecker, and Paul Dendrenos have assisted with station support at DSS 14 on many occasions. Ray Jurgens provided insights and suggested new approaches during the exploration of the new display. Paul Willis made comments that improved this article.

References

[1] S. D. Howard, "The Real-Time Display of Interferometry Data for Goldstone Radar Astronomy Data-Acquisition," *The Telecommunications and Data Acquisition Progress Report 42-117, vol. January–March 1994*, Jet Propulsion Laboratory, Pasadena, California, pp. 213–227, May 15, 1994.

[2] E. R. Tufte, *The Visual Display of Quantitative Information*, Cheshire, Connecticut: Graphics Press, 1983.

[3] S. D. Howard, "Improving a Data-Acquisition Software System With Abstract Data Type Components," *The Telecommunications and Data Acquisition Progress Report 42-100, vol. October–December 1989*, Jet Propulsion Laboratory, Pasadena, California, pp. 248–251, February 15, 1990.

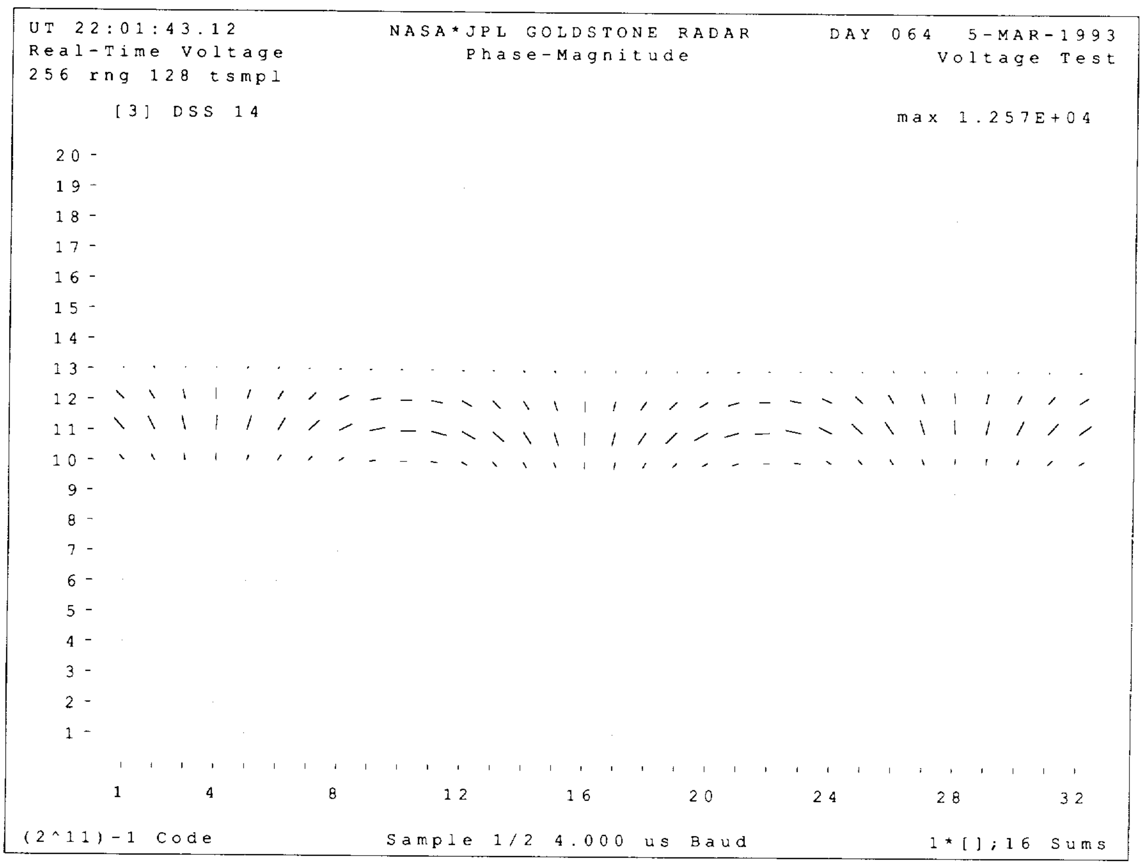

Fig. 1. Normal loop-back test of oversampled configuration.

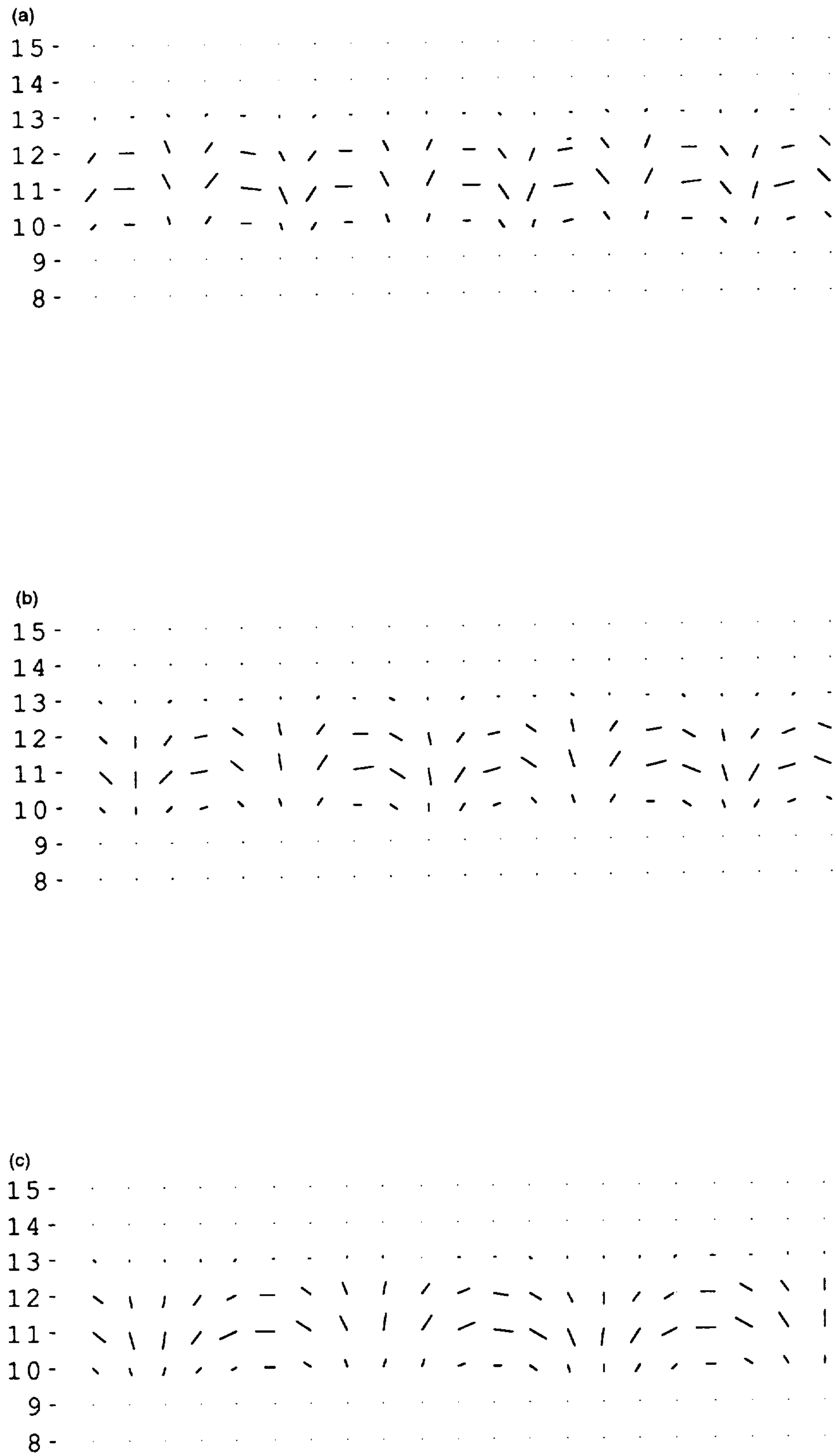

Fig. 2. Normal oversampled loop-back test at (a) 20, (b) 15, (c) 10, (d) 5, (e) 0, and (f) –5 Hz.

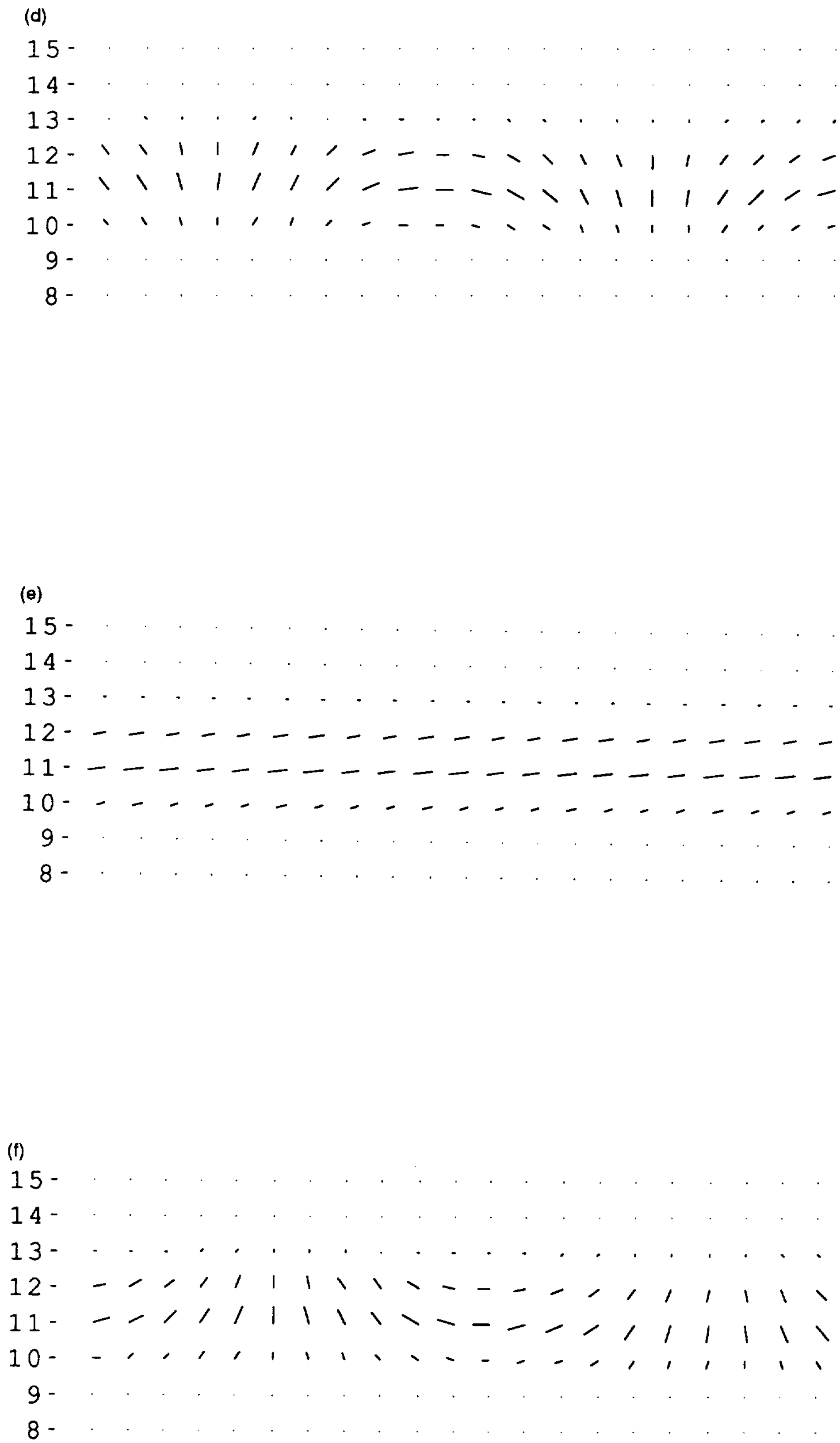

Fig. 2. (Cont'd)

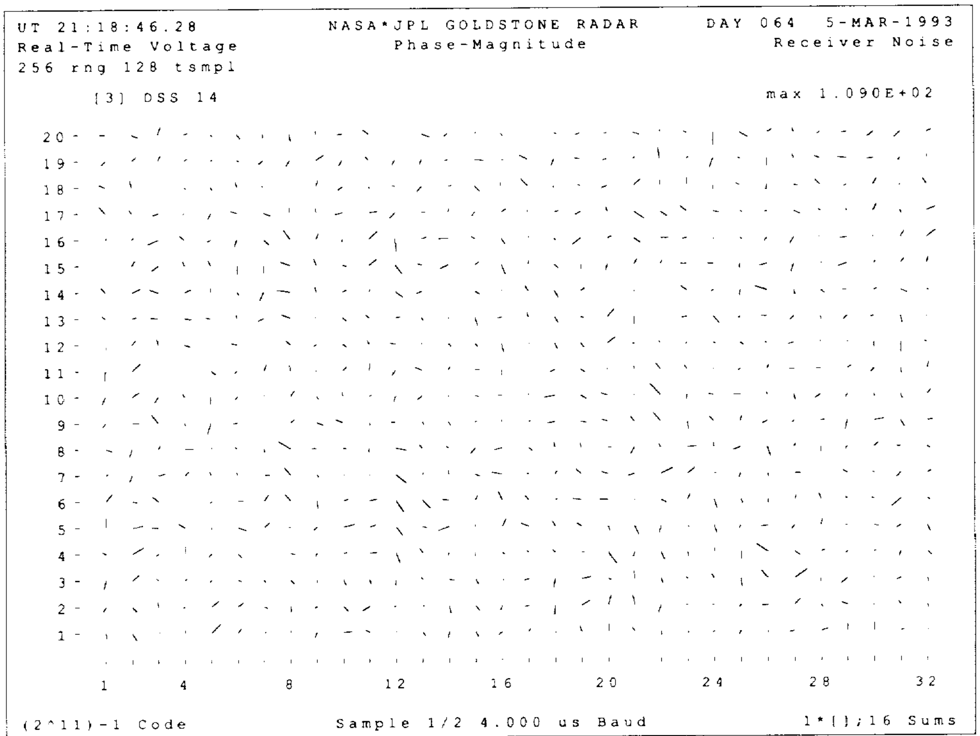

Fig. 3. Gaussian noise.

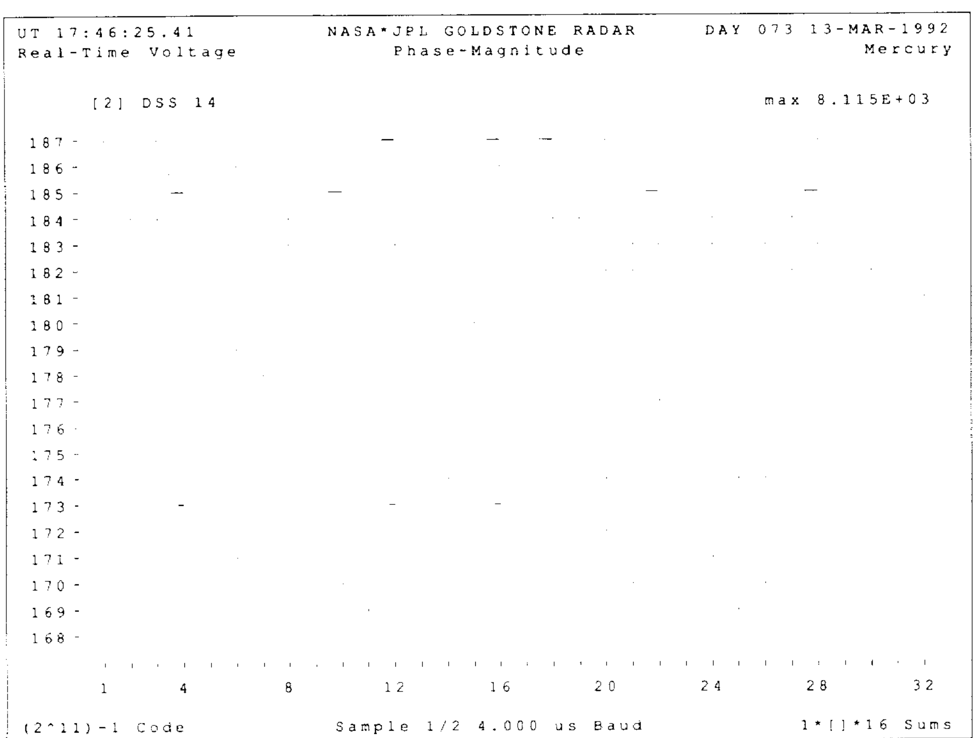

Fig. 4. Evidence of a memory failure in a correlator–accumulator module.

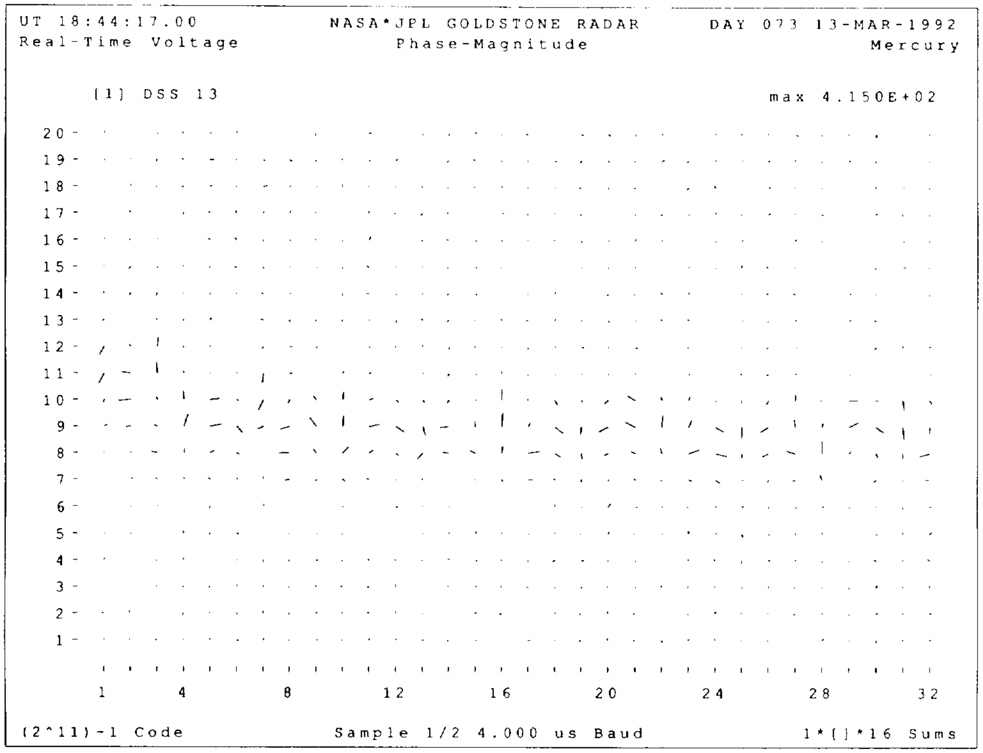

Fig. 5. Analog-to-digital converter adjustment problem.

N94-35562

TDA Progress Report 42-117

May 15, 1994

A 32-GHz Solid-State Power Amplifier for Deep Space Communications

P. D. Wamhof, D. L. Rascoe, K. A. Lee, and F. S. Lansing
Spacecraft Telecommunications Equipment Section

A 1.5-W solid-state power amplifier (SSPA) has been demonstrated as part of an effort to develop and evaluate state-of-the-art transmitter and receiver components at 32 and 34 GHz for future deep space missions. Output power and efficiency measurements for a monolithic millimeter-wave integrated circuit (MMIC)-based SSPA are reported. Technical design details for the various modules and a thermal analysis are discussed, as well as future plans.

I. Introduction

The Deep Space Network is developing telecommunication capability at 32 GHz (Ka-band) with expected improvement of as much as 8 dB over the current performance at 8 GHz (X-band). A proof-of-concept 32-GHz solid-state power amplifier (SSPA) with an output power of 1.56 W has been designed and demonstrated for future spacecraft applications.

The objective was to demonstrate useful RF output power of greater than 1.5 W with an efficiency greater than 15 percent at 32 GHz. We also wanted to use state-of-the-art components that were readily available from vendors and to build a compact system that could be interfaced with the deep space transponder.

The development of this SSPA provided practical hands-on experience in the incorporation of Ka-band monolithic millimeter-wave integrated circuits (MMICs) into an amplifier architecture. Other useful information was obtained in the areas of mechanical and electronic system integration and high-power RF testing. The completed hardware from this effort is currently being used as a stepping stone toward 32-GHz SSPAs having higher efficiencies (>25 percent) and output power capacity (1.7 W).

II. Subsystem Design

Some initial goals and requirements for the 32-GHz SSPA were established based upon future deep space mission requirements. An RF output power level of 1.5 W having greater than 15 percent power added efficiency was selected, which would make the SSPA a good candidate for insertion into the Pluto Fast Flyby mission. The SSPA would also require 31 dB of RF gain in order to interface with the deep space transponder that provides 1 mW of input power to the SSPA.

We surveyed industry to find 32-GHz high-power devices (>0.5 W) having efficiencies greater than 25 percent in order to meet these requirements and came up with three possible vendors. GE Aerospace has 1.0-W 32-GHz pseudomorphic high electron-mobility transistor (PHEMT) discrete devices with 30 percent power added efficiency, but these were not available for use outside of GE Aerospace. Raytheon initially claimed to have